Virtual Axis Finder: A New Method to Determine the Two Kinematic Axes of Rotation for the Tibio-Femoral Joint

Michelle Roland
Biomedical Engineering Program,
One Shields Ave.,
University of California,
Davis, CA 95616

M. L. Hull[1]
Biomedical Engineering Program and
Department of Mechanical Engineering,
One Shields Ave.,
University of California,
Davis, CA 95616
e-mail: mlhull@ucdavis.edu

S. M. Howell
Department of Mechanical Engineering,
One Shields Ave.,
University of California,
Davis, CA 95616

*The tibio-femoral joint has been mechanically approximated with two fixed kinematic axes of rotation, the longitudinal rotational (LR) axis in the tibia and the flexion-extension (FE) axis in the femur. The mechanical axis finder developed by Hollister et al. (1993, "The Axes of Rotation of the Knee," Clin. Orthop. Relat. Res., **290**, pp. 259–268) identified the two fixed axes but the visual-based alignment introduced errors in the method. Therefore, the objectives were to develop and validate a new axis finding method to identify the LR and FE axes which improves on the error of the mechanical axis finder. The virtual axis finder retained the concepts of the mechanical axis finder but utilized a mathematical optimization to identify the axes. Thus, the axes are identified in a two-step process: First, the LR axis is identified from pure internal-external rotation of the tibia and the FE axis is identified after the LR axis is known. The validation used virtual simulations of 3D video-based motion analysis to create relative motion between the femur and tibia during pure internal-external rotation, and flexion-extension with coupled internal-external rotation. The simulations modeled tibio-femoral joint kinematics and incorporated 1 mm of random measurement error. The root mean squared errors (RMSEs) in identifying the position and orientation of the LR and FE axes with the virtual axis finder were 0.45 mm and 0.20 deg, and 0.11 mm and 0.20 deg, respectively. These errors are at least two times better in position and seven times better in orientation than those of the mechanical axis finder. Variables, which were considered a potential source of variation between joints and/or measurement systems, were tested for their sensitivity to the RMSE of identifying the axes. Changes in either the position or orientation of a rotational axis resulted in high sensitivity to translational RMSE (6.8 mm of RMSE per mm of translation) and rotational RMSE (1.38 deg of RMSE per degree of rotation), respectively. Notwithstanding these high sensitivities, corresponding errors can be reduced by segmenting the range of motion into regions where changes in either position or orientation are small. The virtual axis finder successfully increased the accuracy of the mechanical axis finder when the axes of motion are fixed with respect to the bones, but must be used judiciously in applications which do not have fixed axes of rotation.*
[DOI: 10.1115/1.4000163]

Keywords: knee, kinematics, axis, rotation, error analysis, simulation, motion analysis

1 Introduction

Modeling knee kinematics has been heavily studied in the biomechanics literature because it aids in clinical diagnostics [1–4], helps understand sport injury mechanisms [5,6], and is essential in developing new joint prosthetics and arthroplasties [3,7–9]. Furthermore, modeled kinematics have been shown to be sensitive to the selection of the rotational axes [10–14], so the position and orientation of joint rotational axes must be accurately determined to properly model joint kinematics. Accordingly, it is important to develop an accurate method of defining a rotational axis model under a variety of conditions.

Several methods for defining rotational axes have been described in the literature, however each has its limitations. One method for finding the axes is a mechanical axis finder, however, there is an error of 1 mm in translational positioning and 1.5 deg in rotational positioning [15]. A second method used the compound hinge model [16], however the mathematical description of the technique was too limited to evaluate the reliability of the method. A third method found two rotational axes from coupled rotations in the ankle [4], but the technique has not been applied to the knee. While this technique accurately identifies the ankle's rotational axes, it requires at least 25 deg of rotation to occur about both axes simultaneously, which is not applicable to the knee joint because of the limited internal-external rotation during bending. Thus, there remains a need for a quantitative and mathematically clear method of determining the two rotational axes in the tibio-femoral joint.

The application of the mechanical axis finder showed that decoupling the flexion-extension and internal-external rotations of the knee joint during bending is a viable method of identifying and describing knee kinematics [15]. However, the major source of error in this technique was the visually-based alignment of the axis finder to the rotational axes. Thus, one objective was to render the axis finder concept more objective by creating a virtual axis finder that utilizes a mathematical optimization in conjunction with simulated experimental data which are representative of tibio-femoral kinematics reported in the literature to identify the flexion-extension (FE) and longitudinal rotation (LR) axes. By

[1]Corresponding author.

Contributed by the Bioengineering Division of ASME for publication in the JOURNAL OF BIOMECHANICAL ENGINEERING. Manuscript received March 3, 2009; final manuscript received June 30, 2009; accepted manuscript posted September 4, 2009; published online December 18, 2009. Editor: Michael Sacks.

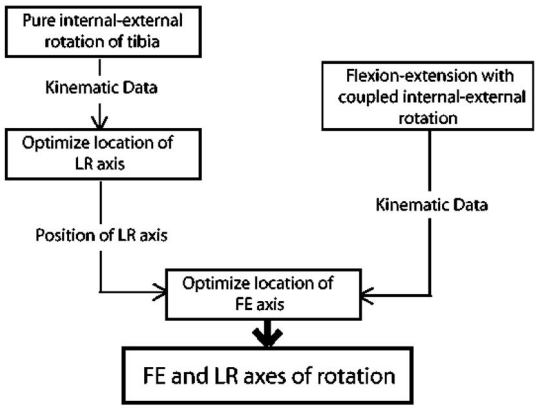

Fig. 1 Flow chart representing the sequence of steps for the virtual axis finder

changing the implementation of the axis finder from being a visually-based procedure to being a mathematical optimization, our goal was to improve the error.

A second objective was to validate the virtual axis finder. A number of variables, such as random error in the kinematic data and range of internal-external rotation may differ between measurement modalities and/or condition of the knee. Because these variables can affect the accuracy of the method, it was of interest in the validation to conduct a sensitivity analysis for each variable using the bias, precision, and root mean square (rms) of the error in locating the LR and FE axes as dependent variables.

2 Methods

Although the validation of the method presented here was performed virtually, the method was developed to be applied specifically to a tibio-femoral joint. Therefore, anatomic references and figures are used here to guide the application of this virtual validation to an actual tibio-femoral joint. All points, coordinate systems, and motions were created virtually such that they represented the anatomy and kinematics of an actual tibio-femoral joint.

The virtual axis finder mimics the methodology of the mechanical axis finder [15] by identifying the LR and FE axes in a two-step process. The first step identifies the LR axis from pure internal-external rotation of the tibia at several flexion angles. The second step identifies the FE axis from unconstrained flexion-extension with coupled internal-external rotation. Because the LR axis is already identified, the coupled internal-external rotation which occurs with flexion-extension can be mathematically eliminated.

To increase the accuracy over that of the mechanical axis finding method, the visual-based alignment of the mechanical pin to the axes was eliminated and replaced with a mathematical optimization. Thus, custom software was created which utilizes the input of 3D video-based motion analysis data of the internal-external rotation and unconstrained flexion-extension, and outputs an optimized location of the axes (Fig. 1).

To validate this custom software, simulated 3D video-based motion analysis data were created with a virtual 2 degree-of-freedom kinematic model of the tibio-femoral joint. The model consisted of two nonintersecting, perpendicular, fixed axes of rotation [15,16] and a set of four markers fixed to each axis. Flexion-extension and internal-external rotations that were representative of tibio-femoral rotational kinematics reported in the literature were input into the model and the corresponding three-dimensional positions of the markers rotating about the axes were output. Random measurement noise was added to the marker data to make it realistic.

The derivation of the mathematical optimization utilizes the following nomenclature: a position vector $\mathbf{r}$ expressed in coordinate system a, from point 1 (p1) fixed in one body to point 2 (p2) fixed in another body is expressed in Eq. (1).

$$\mathbf{r_a^{p2/p1}} = x_a^{p2/p1}\hat{\mathbf{i}}_\mathbf{a} + y_a^{p2/p1}\hat{\mathbf{j}}_\mathbf{a} + z_a^{p2/p1}\hat{\mathbf{k}}_\mathbf{a} \tag{1}$$

To describe the relative motion, two coordinate systems were established. The femoral anatomic coordinate system (F) was fixed in the femur. The origin was situated at the midpoint between the medial and lateral epicondylar eminences with $\hat{\mathbf{i}}_\mathbf{F}$ directed anteriorly, $\hat{\mathbf{j}}_\mathbf{F}$ directed medially, and $\hat{\mathbf{k}}_\mathbf{F}$ directed proximally. A similar anatomical coordinate system was fixed in the tibia (T) with the origin situated at the midpoint between the medial and lateral tibial eminences. Both coordinate systems were known at each instant in time in a global coordinate system (G).

2.1 Virtual Axis Finder. The virtual determination of the axes was based on the premise that a rotational axis can be defined by two points fixed in a rotating body, which do not move with respect to the other body. Finding two points on the LR axis (LR1 and LR2) required a nonlinear optimization and an error function (E) which quantified the total relative motion between a point in the tibia (l) and the origin of the femoral anatomic coordinate system (Fo) (Eq. (2)). When any point on the LR axis is selected, E^{LR} goes to zero; therefore, Eq. (2) was minimized two separate times in MATLAB's nonlinear least-squares function to identify the coordinates of two points: LR1 and LR2 in T. Because there are an infinite number of points which exist along the rotational axis, the search spaces for LR1 and LR2 were constrained to two parallel planes: the $\hat{\mathbf{i}}_T\hat{\mathbf{j}}_T$-plane approximately aligned with the tibial plateau (z_T=0 cm), and the $\hat{\mathbf{i}}_T\hat{\mathbf{j}}_T$-plane 15 cm distal to the plateau (z_T=−15 cm), respectively. The total number of data points collected throughout internal-external rotation is represented by n, and the mean value of a variable for n data points is indicated with a bar.

$$E^{\mathrm{LR}} = \sqrt{\frac{1}{n}\sum_{i=1}^{n}(((x_F^{l/Fo})_i - \bar{x}_F^{l/Fo})^2 + ((y_F^{l/Fo})_i - \bar{y}_F^{l/Fo})^2)} \tag{2}$$

The vector from LR2 to LR1 in T ($\mathbf{r_T^{LR1/LR2}}$) marked the position of the LR axis (Fig. 2). The full derivation of the error function can be found in the Appendix.

To identify the FE axis, two points fixed in the femur (FE1 and FE2) which did not move with respect to the tibia had to be identified. However, it was not possible to search from any random point fixed in the tibia because of the natural internal-external rotation, which occurs during flexion-extension [15–17]. To eliminate the movement of the selected point during the coupled rotations, the position vectors utilized in the error functions were from a point on the LR axis to two points fixed in the femur. Because the tibia's coordinate system rotates relative to the femur, the components of the vector are constantly shifting when a point on the FE axis is selected; however, the magnitude of the vector remains constant. Thus, the error function E^{FE} used to determine two points on the FE axis from natural flexion-extension coupled with internal-external rotations utilized the change in the magnitude of a vector from a point on the LR axis (LR) to a point (f) fixed in the femur (Eq. (3)). The search spaces for FE1 and FE2 were confined to two parallel planes: the $\hat{\mathbf{i}}_F\hat{\mathbf{k}}_F$-plane containing the medial epicondylar eminence (y_F=−5 cm), and the $\hat{\mathbf{i}}_F\hat{\mathbf{k}}_F$-plane containing the lateral epicondylar eminence (y_F=5 cm), respectively (Fig. 3). Here, n indicates the total number of data points collected throughout flexion-extension.

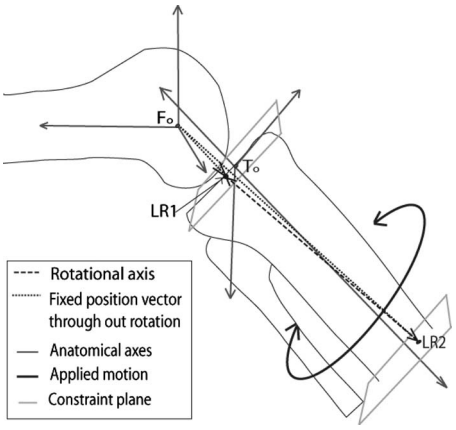

Fig. 2 A schematic shows the coordinate systems used to determine the LR axis of rotation (line from LR1 to LR2). From the motion that resulted from an applied internal-external rotational moment on the tibia, two points (LR1,LR2) were identified in the tibia that did not move with respect to the femur: LR1 is constrained to a plane in the tibia which was adjacent to the tibial plateau, and LR2 is constrained to a plane in the tibia distal to the tibial plateau. Fo is the origin of the femoral anatomic coordinate system which is fixed in the femur. To is the origin of the tibial anatomic coordinate system fixed in the tibia.

$$E^{\mathrm{FE}} = \sqrt{\frac{1}{n}\sum_{i=1}^{n}\left(|\mathbf{r}_{\mathbf{T}}^{\mathbf{f/LR}}|_i - |\bar{\mathbf{r}}_{\mathbf{T}}^{\mathbf{f/LR}}|\right)^2} \tag{3}$$

The vector from the medial point on the FE axis (FE1) to the lateral point on the FE axis (FE2) in F ($\mathbf{r}_{\mathbf{F}}^{\mathbf{FE2/FE1}}$) marked the position of the FE axis. The full derivation of the error function is in the Appendix.

Because $\mathbf{r}_{\mathbf{T}}^{\mathbf{LR1/LR2}}$ and $\mathbf{r}_{\mathbf{F}}^{\mathbf{FE2/FE1}}$ were described in anatomically relevant coordinate systems, the orientations of the axes were described with clinically relevant projection angles onto anatomical planes and the positions were described by coordinates of the intersection of the axis with the plane containing the coordinate system origin. The orientation of the LR axis was defined with the projection angle of $\mathbf{r}_{\mathbf{T}}^{\mathbf{LR1/LR2}}$ onto the $\hat{\mathbf{i}}_{\mathbf{T}}\hat{\mathbf{k}}_{\mathbf{T}}$-plane (flexion-extension orientation) and $\hat{\mathbf{j}}_{\mathbf{T}}\hat{\mathbf{k}}_{\mathbf{T}}$-plane (varus-valgus orientation). The anterior-posterior ($x_T^{\mathrm{LR1}/To}$) and medial-lateral ($y_T^{\mathrm{LR1}/To}$) components of $\mathbf{r}_{\mathbf{T}}^{\mathbf{LR1/To}}$ defined the position of the LR axis. Similarly, the orientation of the FE axis was defined by the projection angle of $\mathbf{r}_{\mathbf{F}}^{\mathbf{FE1/FE2}}$ onto the $\hat{\mathbf{i}}_{\mathbf{F}}\hat{\mathbf{j}}_{\mathbf{F}}$-plane (internal-external orientation) and $\hat{\mathbf{i}}_{\mathbf{F}}\hat{\mathbf{k}}_{\mathbf{F}}$-plane (varus-valgus orientation). The point midway between FE1 and FE2 was utilized to describe the position of the FE axis because this point lies in the sagittal plane that contains the origin of the femoral coordinate system. Therefore, the medial-lateral ($y_F^{\frac{(\mathrm{FE1+FE2})}{2}/Fo}$) and proximal-distal ($z_F^{\frac{(\mathrm{FE1+FE2})}{2}/Fo}$) components of the vector from Fo to the midway point ($\mathbf{r}_{\mathbf{F}}^{\frac{\mathbf{(FE1+FE2)}}{\mathbf{2}}\mathbf{/Fo}}$) defined the position of the FE axis. Thus, there were four clinically relevant dependent variables that described the orientation and position of each axis.

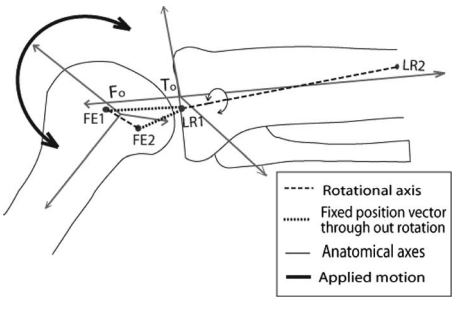

Fig. 3 A schematic represents the coordinate systems used to determine the FE axis of rotation (line from FE1 to FE2). With an applied flexion-extension rotation of the femur, the tibia will naturally internally and externally rotate. Therefore, the search for two position vectors whose magnitudes do not change during the rotation was initialized from a point on the LR axis (LR1). The search for the first point, FE1, is constrained to a plane fixed in the femur which contains the medial epicondylar eminence. The search for the second point, FE2, is constrained to a plane fixed in the femur which contains the lateral epicondylar eminence. Fo is the origin of the femoral anatomic coordinate system which is fixed in the femur. To is the origin of the tibial anatomic coordinate system fixed in the tibia.

Table 1 The test variables and their ranges which were examined in the validation of the virtual axis finder

Variable	Range	Increments	Baseline conditions
Standard deviation of random error (mm)	0–10	1	1
Range of internal-external motion (deg)	5–45	5	20
Translation of LR axis (mm)	0–20	5	0
Rotation of LR axis (deg)	0–5	1	0
Error in LR1 ($x_T^{\mathrm{LR1}/To}, y_T^{\mathrm{LR1}/To}$) (mm, mm)	(0, 0)–(20, 20)	(5, 5)	(0, 0)

2.2 Validation. The virtual axis finder was validated with simulated kinematic data. The simulations were performed in MATLAB 7.4.0. Initially, a simulation was performed on a baseline set of conditions which represented tibio-femoral kinematics that are reported in the literature. Several of these baseline conditions were selected for a sensitivity analysis because they are a potential source of variation, either from knee to knee, or from varying measurement modalities (Table 1).

2.2.1 Baseline Model. The simulations were created under the assumption that 3D video-based motion analysis was used for kinematic data collection. Two sets of four reflective markers were rigidly mounted to the femur and tibia. Each set of markers formed a Cartesian coordinate system with marker 1 defining the origin, marker 2 defining the x-axis, marker 3 defining the y-axis, and marker 4 defining the z-axis. Markers 2–4 were situated 5 cm from marker 1 along their respective axial directions.

The initial positions of the rotational axes were defined with respect to the global coordinate system. Two rotational axis coordinate systems were established: one in the tibia (Ta) and one in the femur (Fa). The LR axis was defined as $\hat{\mathbf{k}}_{\mathbf{Ta}}$, $\hat{\mathbf{j}}_{\mathbf{Ta}}$ was oriented medially, and $\hat{\mathbf{i}}_{\mathbf{Ta}}$ was oriented anteriorly. The origin was situated on the midpoint between the medial and lateral tibial eminences. The FE axis was defined as $\hat{\mathbf{j}}_{\mathbf{Fa}}$, $\hat{\mathbf{i}}_{\mathbf{Fa}}$ was oriented anteriorly, and $\hat{\mathbf{k}}_{\mathbf{Fa}}$ was oriented proximally. The origin was situated at the center point between the medial and lateral epicondylar eminences. The LR axis was positioned perpendicular to the FE axis in the coronal plane but nonintersecting by 1 cm posterior [15,16].

The tibial and femoral markers were virtually mounted with respect to the Ta and Fa coordinate systems, respectively. Tibial marker 1 was positioned 10 cm distal and 5 cm medial from the tibial origin. Femoral marker 1 was positioned 15 cm proximal and 5 cm medial from the femoral origin.

The simulated data provided the motion of the two marker sets in the global coordinate system. A normally distributed random error term with zero mean was independently incorporated into

each marker's data [18]. The precision was set conservatively to 1 mm [19,20].

The range of motion that was simulated was selected from the literature. Pure internal-external rotation under a small applied torque (3 N m) was simulated with 20 deg of internal-external rotation [21]. Natural flexion-extension was simulated with 90 deg of flexion and 15 deg internal rotation of the tibia, which occurred during the first 30 deg of flexion in a manner that emulated the screw home mechanism [16,22,23].

To verify that the global minimum was being determined with the optimization algorithm, a pilot study was performed in which the position of the LR axis was determined on the same set of internal-external rotational data for 100 iterations. For each iteration, the error in the initial guess for the x_T and y_T components of LR1 and LR2 utilized in the optimization routine were independently randomized with a uniform random number generator (from −20 mm to 20 mm). The standard deviations of the optimized position of LR1 and LR2 were determined to be 0.0010 mm and 0.0013 mm, respectively. Thus, the optimization converged to the global minimum. Because the position of the initial guess was not a factor, the error in the initial guess was implemented as a random variable ($\sigma^2=10$ mm, $\mu=0$) throughout the validation.

Pilot studies revealed a large sensitivity to the random error in the marker positions. Therefore, rotational steps were simulated such that stepwise rotation was applied and held for a period of time. By averaging the position of the markers during each rotational step, the random error input into the software was filtered and the resulting error was greatly reduced. It was determined that both the number of rotational steps and the number of data points collected during each step reduced the error in finding the axes. The condition that was selected as the baseline condition for pure internal-external rotation of the tibia was five rotational steps (4 deg of rotation per step) with 500 data points per step (RMSE equal to 0.21 deg and 0.45 mm). The condition selected for natural flexion-extension of the tibia was 15 rotational steps (6 deg of rotation per step) with 500 data points collected per step (RMSE equal to 0.20 deg and 0.11 mm). These parameters were utilized because the RMSE values for the two motions were minimal and an increase in rotational steps did not provide a proportionate reduction in error. Furthermore, the parameters could be reasonably applied to the actual range of motions expected.

For each condition that was simulated, a new randomized data set and randomized initial guess were recreated for 100 iterations. An error (e_i) was determined for each result from

$$e_i = \text{actual-measured}_i \tag{4}$$

To quantify the accuracy of this method, the bias or average error, precision or random error, and RMSE were determined over all 100 iterations within each test condition. The resulting error terms for the two projection angles were statistically pooled together to provide the overall rotational error, and the two translational variables were statistically pooled together to provide the overall translational error.

2.2.2 Test Conditions. Because the amount of random error in the kinematic data can vary from one system to the next [20], it was important to determine the sensitivity of the method to the random error. Therefore, the standard deviation of the random error term was varied from 0 mm to 10 mm in 1 mm increments to quantify the software's sensitivity to the random measurement error.

The amount of pure internal-external rotation of the tibia can vary greatly from knee to knee [21]. Therefore, it was important to understand how the range of motion impacts the accuracy of this method. The error in finding the LR axis was determined from 5 deg to 45 deg of internal-external rotation in 5 deg increments.

Although this method assumes that the axes of rotation are fixed in the bone, this may not be a perfect assumption [16]. Therefore, it was important to quantify the error in determining the axis of rotation when an axis is not perfectly fixed in the bone. This was quantified under two separate conditions: translation and rotation of the LR axis. Pilot studies revealed that the direction of translation and/or rotation did not affect the magnitude of the errors; therefore, only one translational direction and one rotational direction were studied. To quantify the error from translating an axis of rotation, the instantaneous position of the LR axis was translated along the initial orientation of $\hat{\mathbf{i}}_{\mathbf{Ta}}$. The magnitude of the translation ranged from 0 mm to 20 mm of translation in 5 mm increments. To quantify the error from rotating the axis of rotation, the instantaneous orientation of the LR axis was rotated about the initial orientation of $\hat{\mathbf{i}}_{\mathbf{Ta}}$. The rotation of the axis' orientation ranged from 0 deg to 5 deg of rotation in 1 deg increments. The translations and rotations of the LR axis were proportionately distributed throughout the 20 deg of internal-external rotation. The error term was calculated by subtracting the measured axis from the average position and orientation of the axis.

Because this method requires that the LR axis is determined before the FE axis can be determined, any error in the LR axis could be propagated when determining the FE axis. Therefore, the error in the FE axis was quantified after errors in the position of LR1 were implemented. An error term was incorporated into the $x_T^{\mathrm{LR1}/To}$ and $y_T^{\mathrm{LR1}/To}$ components of the vector $\mathbf{r}_{\mathbf{T}}^{\mathbf{LR1/To}}$ in Eqs. (A13) and (A14), and the resulting error in the FE axis was quantified. The error term was varied from 0 mm to 20 mm in 5 mm increments.

3 Results

The rotational and translational RMSE for the orientation and position of the LR axis at the baseline conditions (Table 1) were 0.21 deg and 0.45 mm, respectively. The rotational and translational RMSE of the orientation and position of the FE axis at the baseline conditions (Table 1) with 90 deg flexion and 15 deg of coupled internal rotation were 0.20 deg and 0.11 mm, respectively.

Increasing the standard deviation of the random error term linearly increased the rotational and translational RMSE of the orientation and position of the LR axis at a rate of 0.20 deg of RMSE per mm of random error ($R^2=0.994$) and 0.45 mm of RMSE per mm of random error ($R^2=0.997$), respectively. The precision increased at a similar rate while the bias was negligible (Fig. 4).

The rotational and translational RMSE of the LR axis decreased quadratically as the range of motion increased. With 20 deg of rotation, the rotational and translational RMSE dropped to 0.21 deg and 0.45 mm, respectively. The bias was negligible (Fig. 5).

Translating and rotating the axis of rotation throughout the 20 deg range of internal-external rotation caused the most drastic impact on the RMSE of the LR axis. Furthermore, it was the bias which predominantly caused the increase in RMSE rather than the precision. Translating the axis of rotation caused a linear increase in the translational RMSE error at a rate of 6.8 mm of RMSE per mm of translation ($R^2=0.998$). The rotational RMSE remained constant at approximately 0.2 deg, which is equivalent to the baseline error for the LR axis stated above; therefore, this error was considered negligible. Rotating the axis of rotation caused a linear increase in the rotational error at a rate of 1.38 deg of RMSE per degree of rotation ($R^2=1$). The translational RMSE remained constant at approximately 0.4 mm, which is equivalent to the baseline error stated above; therefore, this error was considered negligible (Fig. 6).

The error in determining the FE axis which results from an input error in the position of LR1 was relatively low. The rotational RMSE for determining the orientation of the FE axis increased at a rate of 0.05 deg of RMSE per mm of error in the position of LR1 ($R^2=0.971$). The translational RMSE was relatively constant at approximately 0.12 mm, which is nearly equivalent to the baseline error for the FE axis; therefore, this error was considered negligible (Fig. 7).

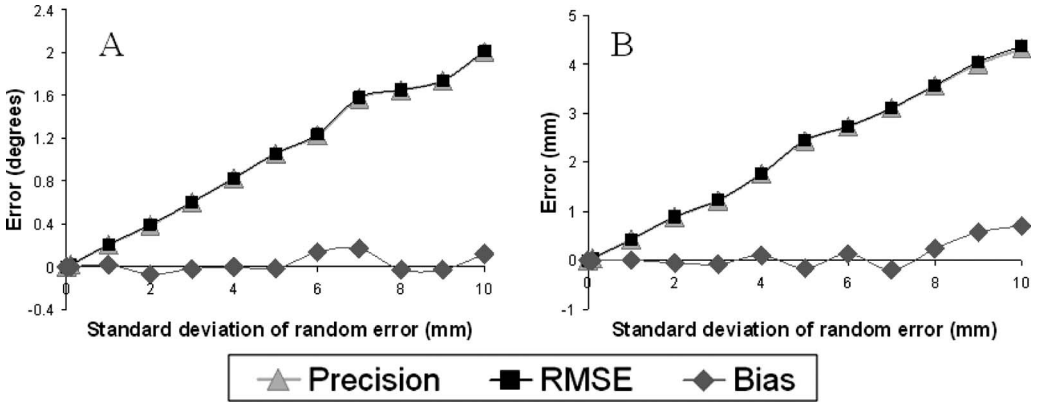

Fig. 4 The RMSE, precision, and bias in determining the LR axis as the random measurement error increases. (A) The pooled rotational errors and (B) the pooled translational errors. The rotational and translational RMSE for the LR axis at the baseline condition of σ=1 mm was 0.21 deg and 0.45 mm, respectively.

4 Discussion

Kinematic models of the tibio-femoral joint aid in clinical diagnostics, sport injury mechanisms, and the development of prosthetics and arthroplasties. Because the accurate identification of the rotational axes utilized in kinematic models can have a significant affect on their applicability, the objectives of this work were to develop and validate a method to determine the kinematic axes of rotation of the tibio-femoral joint. The virtual axis finder was developed such that it utilized the concepts of the mechanical axis finder [15] but eliminated the visual-based alignment method by implementing a mathematical optimization. The validation of the virtual axis finder provided several important indications of this method's capabilities. First, the errors in identifying the LR and FE axes of rotation with the virtual axis finder under parameters that represent expected physical conditions of a tibio-femoral joint were 0.20 deg and 0.45 mm, and 0.20 deg and 0.11 mm, respectively. Second, the only variable which had a nonlinear relationship with the RMSE was the range of internal-external rotation, which caused an exponential decrease in rotational and translational RMSE as the range of rotation increased. However, even the highest errors reported with a small range of rotation were satisfactory. Finally, the translation and rotation of the LR axis had the largest linear sensitivities with the translational and rotational RMSE, respectively. Furthermore, the change in RMSE was predominantly due to an increased bias rather than the precision. Thus, it is this variable which requires careful consideration.

There are several methods in the literature that identify the kinematic axes of the tibio-femoral joint [15,16]. However, the only method which reports errors in a manner that is comparable to the baseline conditions examined here is the mechanical axis finder. Hollister et al. [15] reported a 1 mm and 1.5 deg error in identifying a single axis of rotation. Thus, the virtual axis finder reduced the error in identifying the orientation and position of a single axis of rotation by 55% and 86%, respectively.

Because knee joints have varying internal-external rotational laxities [21], it is important that this method is capable of accurately identifying the LR axis from minimal amounts of internal-external rotation. At full extension, the range of pure internal-external rotation from a ± 3 N m torque can be as low as 10 deg [21]. The results reported here indicate that with 10 deg of internal-external rotation, the rotational and translational RMSE is 0.41 deg and 0.85 mm, respectively, which is less than the errors reported for the mechanical axis finder [15]. Thus, the virtual axis finder will identify the LR axis more accurately than the mechanical axis finder despite the amount of internal-external rotational laxity of each individual tibio-femoral joint.

This method was developed on the assumption that the axes of rotation are fixed in the bone. Any translation and/or rotation of

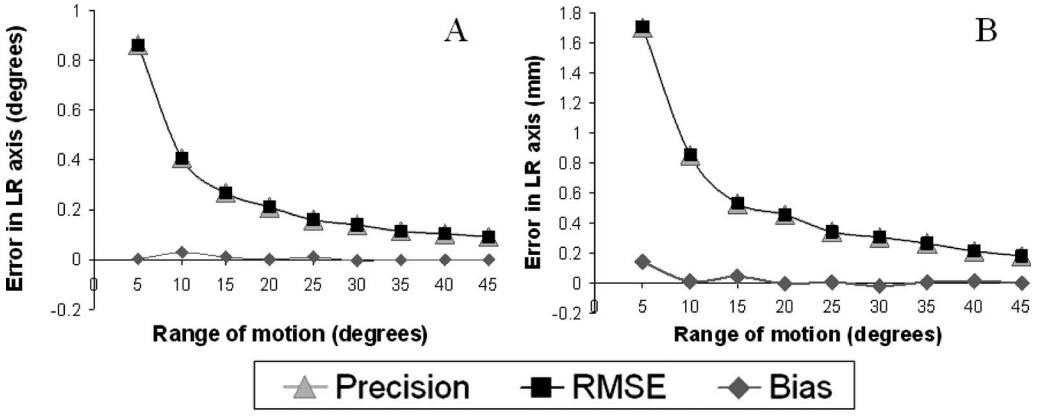

Fig. 5 The RMSE, precision, and bias in identifying the LR axis which results from varying levels of internal-external tibial rotation. (A) The pooled rotational errors and (B) the pooled translational errors. The rotational and translational RMSE for the LR axis at the baseline condition of 20 deg was 0.21 deg and 0.45 mm, respectively.

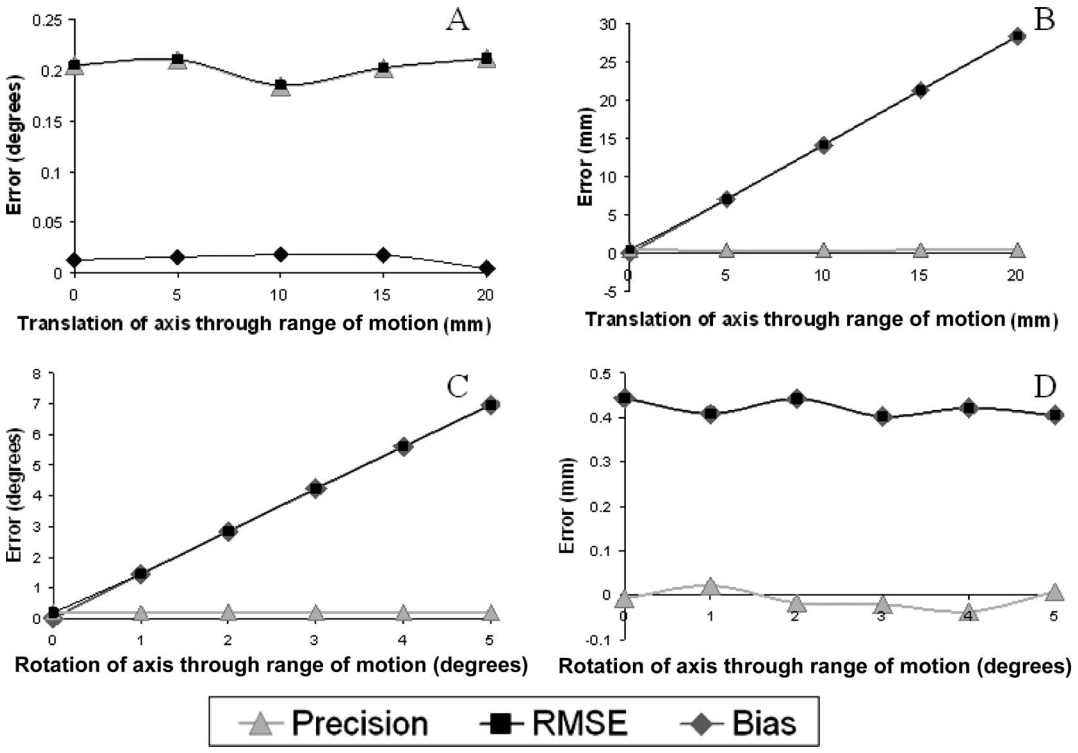

Fig. 6 The RMSE, precision, and bias which results from determining the position of the LR axis when its position (A) and (B), or orientation (C) and (D) does not stay fixed. (A) and (C) The pooled rotational error, and (B) and (D) the pooled translation errors. Note that the RMSE in (A) and (D) are nearly equivalent to the baseline RMSE for the LR axis. Thus, the error is due to the random error term in the data rather than the translation and/or rotation of the LR axis.

the rotational axis alters the motion of the markers in a plane perpendicular to the rotational axis, and consequently changes the apparent radius of curvature. This change in the radius of curvature causes the optimized center point of that motion to shift, resulting in a measurement bias. Hence, translation and rotation of the LR axis caused the greatest increase in the bias and RMSE of identifying the LR axis. However, it is important to note that given a constant translation or rotation per degree of axial rotation, the RMSE of identifying an unfixed axis of rotation is smaller when there is a greater range of motion. Thus, the virtual axis finder should be less sensitive to an unfixed FE axis of rotation than reported here for the LR axis because this degree of freedom has a larger range of motion than internal-external rotation.

Because the assumption of fixed axes of rotation may not be valid for every application and because this method is sensitive to this assumption (Fig. 6), it is important to have an alternative approach for applications which may not have fixed axes. The

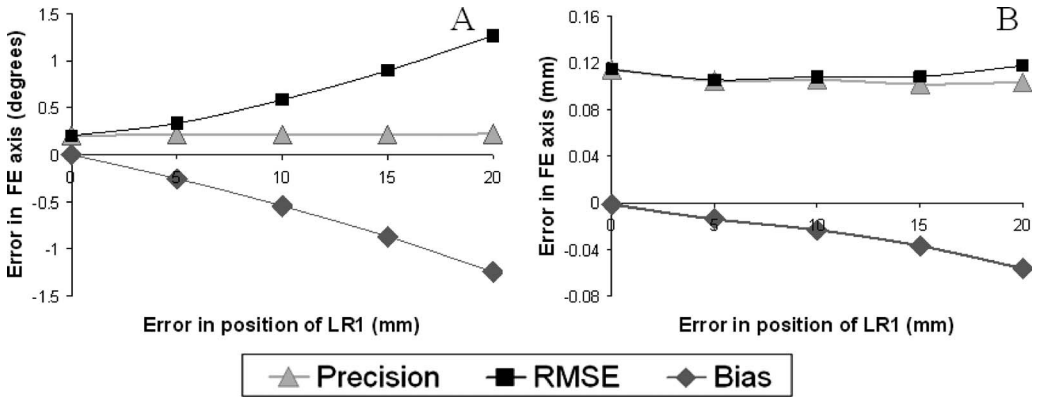

Fig. 7 The RMSE, precision, and bias for determining the FE axis after an error in the position of LR1 was incorporated into the optimization. (A) The pooled rotational errors and (B) the pooled translational errors. Note that the nonzero rotational and translational RMSE reported for 0 mm of input error in the position of LR1 equates to the baseline error for determining the FE axis given 90 deg of flexion with 15 deg of internal rotation and a random error term (σ=1 mm, μ=0).

virtual axis finder had a lower RMSE for small range of motion (Fig. 5) than for unfixed axes (Fig. 6); therefore, the total range of motion can be shortened or partitioned until the assumption of fixed axes is valid within the partitioned range of motion.

Another assumption used in this virtual validation concerns the orientation that was established between the bone coordinate systems (F and T) that were defined by the global position of the virtual markers and the coordinate systems utilized to establish the rotational axes (Fa and Ta). For simplicity, these two coordinate systems were aligned such that the defined rotational axes, FE and LR, were collinear with one of the axes of F and T, respectively. In practice, this will not be the case. Actual markers will not be fixed to the bones such that at least two markers are positioned directly on the rotational axis allowing the bone coordinate system to align with the rotational axis. It is possible that when the bone coordinate system is skewed from the orientation of the rotational axis, the virtual axis finder will not be able to optimize the location of the rotational axis with the same precision. However, if the bone coordinate system is redefined in an anatomically relevant manner such that one axis is approximately aligned with the rotational axis, then errors introduced from skewing the bone coordinate system from the rotational axis can be reduced. Thus, three anatomic landmarks in each bone should be digitized with respect to the bone markers to define the appropriate transformation from the marker-based coordinate system to an anatomically-based coordinate system. To approximately align an axis in each bone with the corresponding rotational axes, the femoral coordinate system must be approximately aligned to the transepicondylar axis and the tibial coordinate system must be approximately aligned with the long axis of the tibia. Because these anatomic axes are approximately aligned with the FE and LR rotational axes respectively [15,16], the potential error introduced from bone markers that are skewed with respect to the rotational axes will be reduced.

The use of rotational steps, which were statically held for a period of time at each angular position, introduces potential challenges for implementing this method. Because it is important that there is no motion during each rotational step, because the number of steps utilized increases the accuracy of this method, and because there is limited range of motion for pure internal-external rotations, this method may require equipment which can control the rotation of the specimens within 1 deg. Any motion which occurs during each step must be minimized and the rotation between each step should be proportionately spaced.

An important aspect of the virtual axis finder is the production of pure internal-external rotation of the tibia about its LR axis. Several methods can be used to accomplish this task in vivo and in vitro. Hollister et al. [15] produced the internal-external rotational moment manually to identify the LR axis. The accurate determination of the LR axis from this method was verified by attaching diodes to the LR axis and tracking their motion during unconstrained flexion-extension. Because the diodes traced concentric circles in a plane perpendicular to the FE axis, it was concluded that the LR axis was accurately identified from the manual rotation. Thus, manually applying an internal-external moment on the tibia should produce pure internal-external rotation about the LR axis with an accuracy which is similar to the results reported for the mechanical axis finder. However, this motion can be produced more precisely through the use of a load application system which can apply an internal-external torque that has an adjustable orientation with respect to the tibio-femoral joint [24–26]. If a rotational torque is applied perfectly about the LR axis of the tibia, then all anterior-posterior and medial-lateral coupled translations of the joint should go to zero. Thus, by adjusting the rotational axis of the machine with respect to the tibia until the coupled translations are minimized, pure internal-external rotation can be produced [24].

Although this validation simulated 3D video-based motion analysis as the measurement modality, the virtual axis finder can be utilized with any three-dimensional kinematic measurement modality. For instance, electromagnetic sensors, roentgen stereophotogrammetric analysis (RSA), and CAD model-based shape matching techniques all could be used to quantify the relative motion between the tibia and femur. Because this validation assumed the markers were rigidly fixed to the bones, it is important that the markers utilized in any application of this method are also rigidly fixed in the bone. Therefore, 3D video markers and/or electromagnetic markers are applicable primarily with cadaveric specimens. Shape matching and RSA, on the other hand, could be utilized in clinical studies.

The benefit of using 3D video markers or electromagnetic sensors is that they can be rigidly fixed to the bones of cadaveric specimens before any surgical alterations have been performed on the joint. This enables tests to be performed on healthy, intact specimens and those results compared with the same joint after an alteration to that joint has occurred. For instance, a new surgical alignment technique for total knee arthroplasty has recently been developed and utilized [27]. This technique attempts to restore the kinematic axes of the pre-arthritic tibio-femoral joint; however, there is no data to support this claim. The virtual axis finder could be utilized to determine how well this alignment goal is achieved in cadaveric specimens.

Many applications of the virtual axis finder are possible with kinematic data collected with CAD model-based shape matching techniques. This technique superimposes the two-dimensional shape of an implanted component on the two-dimensional shape of that component in two separate radiographic or fluoroscopic images [28–30]. By superimposing both images, the three-dimensional position of that component and/or bone can be reconstructed. Shape matching is commonly used to study the kinematics of total knee arthroplasties by shape matching the femoral and tibial components [28,31,32]. Because the virtual axis finder utilizes three points fixed in each bone to define two coordinate systems and ultimately quantify the relative motion between the bones, three identifiable points must be established in the femoral and tibial components [33,34]. Thus the relative position and orientation between the femoral and tibial components can be determined at proportionate intervals throughout internal-external rotation, and unconstrained flexion to determine the rotational axes of a knee after a total knee arthroplasty has been performed. One application of the CAD model-based shape matching technique and the virtual axis finder would be to compare the rotational axes of the two alignment methods available for total knee arthroplasty: traditional mechanical axis alignment [35,36] and kinematic alignment [27]. Many patients have had bilateral total knee arthroplasty (TKA) procedures: one knee with traditional mechanical axis alignment, and one knee with kinematic alignment. Therefore, the virtual axis finder could be utilized on both knees, and a comparison in the rotational axes between the two alignment methods could be obtained.

RSA also provides a unique set of applications with the virtual axis finder. This technique utilizes small tantalum markers which are rigidly inserted into a bone to track the three-dimensional position of that bone from two simultaneous radiographic images [37]. If the beads were inserted into a patient during surgery, then postoperative rotational kinematics could be tracked with the virtual axis finder by X-raying the bones at proportionate intervals throughout the prescribed rotations. One application of RSA would be to measure the change in the rotational axes over time following an anterior cruciate ligament reconstruction. Because it has been determined that the anterior cruciate reconstructions can lengthen in the months following the reconstruction [38], this technique could be utilized to determine whether this lengthening affects the position and/or orientation of the rotational axes.

By employing the methods developed by the mechanical axis finder and implementing a mathematical optimization, the virtual axis finder has advanced tibio-femoral kinematic modeling which should prove useful in a variety of applications. The thorough validation of this method in a virtual setting with respect to a

variety of factors reported here provides researchers with the ability to appropriately apply this method to their specific applications. An application of interest to our research group is to use the virtual axis finder in a cadaveric study to quantify how well the kinematic axes are restored with TKA. We plan to perform this study and report on this in a subsequent paper. Because the virtual axis finder has the capability to quantify and compare the rotational kinematics under a variety of knee conditions and with a variety of measurement modalities, it can become a useful tool in the field of knee biomechanics.

Acknowledgment

We acknowledge the support of the OtisMed Corporation in our research program on total knee arthroplasty.

Appendix: Derivation of the Error Functions for the Virtual Axis Finder

The rotational and translational information which converts a position vector expressed in coordinate system 1 to a vector expressed in a coordinate system 2 (Eq. (A1)) is denoted by the transformation matrix $[\mathbf{T_{2/1}}]$. The transformation matrix $[\mathbf{T_{2/1}}]$ is a 4×4 matrix which contains a 3×3 rotational matrix $[\mathbf{R_{2/1}}]$ and a 3×1 displacement vector $\mathbf{r_2^{O_1/O_2}}$ (Eq. (A2)).

$$\mathbf{r_2} = [\mathbf{T_{2/1}}]\cdot\mathbf{r_1} \tag{A1}$$

$$[\mathbf{T_{2/1}}] = \begin{bmatrix} 1 & 0 & 0 & 0 \\ x_2^{O_1/O_2} & \hat{\mathbf{i}}_\mathbf{2}\cdot\hat{\mathbf{i}}_\mathbf{1} & \hat{\mathbf{i}}_\mathbf{2}\cdot\hat{\mathbf{j}}_\mathbf{1} & \hat{\mathbf{i}}_\mathbf{2}\cdot\hat{\mathbf{k}}_\mathbf{1} \\ y_2^{O_1/O_2} & \hat{\mathbf{j}}_\mathbf{2}\cdot\hat{\mathbf{i}}_\mathbf{1} & \hat{\mathbf{j}}_\mathbf{2}\cdot\hat{\mathbf{j}}_\mathbf{1} & \hat{\mathbf{j}}_\mathbf{2}\cdot\hat{\mathbf{k}}_\mathbf{1} \\ z_2^{O_1/O_2} & \hat{\mathbf{k}}_\mathbf{2}\cdot\hat{\mathbf{i}}_\mathbf{1} & \hat{\mathbf{k}}_\mathbf{2}\cdot\hat{\mathbf{j}}_\mathbf{1} & \hat{\mathbf{k}}_\mathbf{2}\cdot\hat{\mathbf{k}}_\mathbf{1} \end{bmatrix} \tag{A2}$$

The transformation matrices $[\mathbf{T_{F/G}}]_t$ and $[\mathbf{T_{T/G}}]_t$ were defined by the kinematic data at each instant in time (t). The inverse matrix reverses the direction of the transformation (Eq. (A3)).

$$[\mathbf{T_{2/1}}] = [\mathbf{T_{1/2}}]^{-1} \tag{A3}$$

Therefore, the relative position of the femur with respect to the tibia could be determined (Eq. (A4)).

$$[\mathbf{T_{F/T}}] = [\mathbf{T_{F/G}}]\cdot[\mathbf{T_{T/G}}]^{-1} \tag{A4}$$

The position of the LR axis is defined by two points fixed with respect to T (Eqs. (A5) and (A6)).

$$\mathbf{r_T^{LR1/To}} = x_T^{\mathrm{LR1}/To}\hat{\mathbf{i}}_\mathbf{T} + y_T^{\mathrm{LR1}/To}\hat{\mathbf{j}}_\mathbf{T} + z_T^{\mathrm{LR1}/To}\hat{\mathbf{k}}_\mathbf{T} \tag{A5}$$

$$\mathbf{r_T^{LR2/To}} = x_T^{\mathrm{LR2}/Ta}\hat{\mathbf{i}}_\mathbf{T} + y_T^{\mathrm{LR2}/Ta}\hat{\mathbf{j}}_\mathbf{T} + z_T^{\mathrm{LR2}/Ta}\hat{\mathbf{k}}_\mathbf{T} \tag{A6}$$

Because it is the change in position of LR1 and LR2 with respect to the femur throughout internal-external rotation that must be minimized, the position vectors $\mathbf{r_T^{LR1/To}}$ and $\mathbf{r_T^{LR2/To}}$ must be transformed from coordinate system T to coordinate system F for each instant in time, t (Eqs. (A7) and (A8)). The subscript, t, denotes that the variable changes with time.

$$\mathbf{r_{Ft}^{LR1/Fo}} = [\mathbf{T_{F/T}}]_t\cdot\mathbf{r_T^{LR1/Fo}} = (x_F^{\mathrm{LR1}/Fo})_t\hat{\mathbf{i}}_\mathbf{F} + (y_F^{\mathrm{LR1}/Fo})_t\hat{\mathbf{j}}_\mathbf{F} + (z_F^{\mathrm{LR1}/Fo})_t\hat{\mathbf{k}}_\mathbf{F} \tag{A7}$$

$$\mathbf{r_{Ft}^{LR2/Fo}} = [\mathbf{T_{F/T}}]_t\cdot\mathbf{r_T^{LR1/Fo}} = (x_F^{\mathrm{LR2}/Fo})_t\hat{\mathbf{i}}_\mathbf{F} + (y_F^{\mathrm{LR2}/Fo})_t\hat{\mathbf{j}}_\mathbf{Fa} + (z_F^{\mathrm{LR2}/Fo})_t\hat{\mathbf{k}}_\mathbf{F} \tag{A8}$$

LR1 and LR2 are positioned on the longitudinal rotational axis when $(\mathbf{r_F^{LR1/Fo}})_t$ and $(\mathbf{r_F^{LR2/Fo}})_t$ do not change over time. Thus, $x_T^{\mathrm{LR1}/To}$, $y_T^{\mathrm{LR1}/To}$, $x_T^{\mathrm{LR2}/To}$, and $y_T^{\mathrm{LR2}/To}$ are iteratively adjusted until the change in $(x_F^{\mathrm{LR1}/Fo})_t$, $(y_F^{\mathrm{LR1}/Fo})_t$, $(z_F^{\mathrm{LR1}/Fo})_t$, $(x_F^{\mathrm{LR2}/Fo})_t$, $(y_F^{\mathrm{LR2}/Fo})_t$, and $(z_F^{\mathrm{LR2}/Fo})_t$ is minimized. The error functions, E^{LR1} and E^{LR2}, quantify the change in $(\mathbf{r_{Fa}^{LR1/Fo}})_t$ and $(\mathbf{r_{Fa}^{LR2/Fo}})_t$ over time as a root mean square error (Eqs. (A9) and (A10)). Here, n indicates the total number of points collected during internal-external rotation.

$$E^{\mathrm{LR1}} = \sqrt{\frac{1}{n}\sum_{i=1}^{n}(((x_F^{\mathrm{LR1}/Fo})_i - \bar{x}_F^{\mathrm{LR1}/Fo})^2 + ((y_F^{\mathrm{LR1}/Fo})_i - \bar{y}_F^{\mathrm{LR1}/Fo})^2 + ((z_F^{\mathrm{LR1}/Fo})_i - \bar{z}_F^{\mathrm{LR1}/Fo})^2)} \tag{A9}$$

$$E^{\mathrm{LR2}} = \sqrt{\frac{1}{n}\sum_{i=1}^{n}(((x_F^{\mathrm{LR2}/Fo})_i - \bar{x}_F^{\mathrm{LR2}/Fo})^2 + ((y_F^{\mathrm{LR2}/Fo})_i - \bar{y}_F^{\mathrm{LR2}/Fo})^2 + ((z_F^{\mathrm{LR2}/Fo})_i - \bar{z}_F^{\mathrm{LR2}/Fo})^2)} \tag{A10}$$

Because $(x_F^{\mathrm{LR1}/Fo})_t$, $(y_F^{\mathrm{LR1}/Fo})_t$, and $(z_F^{\mathrm{LR1}/Fo})_t$ are each functions of $x_T^{\mathrm{LR1}/To}$ and $y_T^{\mathrm{LR1}/To}$, E^{LR1} is minimized by adjusting $x_T^{\mathrm{LR1}/To}$ and $y_T^{\mathrm{LR1}/To}$. Similarly, E^{LR2} is minimized by adjusting $x_T^{\mathrm{LR2}/To}$ and $y_T^{\mathrm{LR2}/To}$.

The position of the FE axis is defined by two points (FE1 and FE2) which are fixed with respect to F (Eqs. (A11) and (A12)).

$$\mathbf{r_F^{FE1/Fo}} = x_F^{\mathrm{FE1}/Fo}\hat{\mathbf{i}}_\mathbf{F} + y_F^{\mathrm{FE1}/Fo}\hat{\mathbf{j}}_\mathbf{F} + z_F^{\mathrm{FE1}/Fo}\hat{\mathbf{k}}_\mathbf{F} \tag{A11}$$

$$\mathbf{r_F^{FE2/Fo}} = x_F^{\mathrm{FE2}/Fo}\hat{\mathbf{i}}_\mathbf{F} + y_F^{\mathrm{FE2}/Fo}\hat{\mathbf{j}}_\mathbf{F} + z_F^{\mathrm{FE2}/Fp}\hat{\mathbf{k}}_\mathbf{F} \tag{A12}$$

Because it is the change in position of FE1 and FE2 with respect to the tibia throughout flexion-extension that must be minimized, the position vectors of FE1 and FE2 must be transformed from coordinate system F to coordinate system T for each instant in time, t. Furthermore, because of the coupled internal-external rotation, the position vectors must go from a point on the LR axis (LR1) to a point fixed in the femur (Eqs. (A13) and (A14)).

$$\mathbf{r_{Tt}^{FE1/LR1}} = [\mathbf{T_{T/F}}]_t\cdot\mathbf{r_F^{FE1/Fo}} - \mathbf{r_T^{LR1/To}} = (x_T^{\mathrm{FE1}/\mathrm{LR1}})_t\hat{\mathbf{i}}_\mathbf{T} + (y_T^{\mathrm{FE1}/\mathrm{LR1}})_t\hat{\mathbf{j}}_\mathbf{T} + (z_T^{\mathrm{FE1}/\mathrm{LR1}})_t\hat{\mathbf{k}}_\mathbf{T} \tag{A13}$$

$$\mathbf{r_{Tt}^{FE2/LR1}} = [\mathbf{Ta_{T/F}}]_t\cdot\mathbf{r_F^{FE2/Fo}} - \mathbf{r_T^{LR1/To}} = (x_T^{\mathrm{FE2}/\mathrm{LR1}})_t\hat{\mathbf{i}}_\mathbf{T} + (y_T^{\mathrm{FE2}/\mathrm{LR1}})_t\hat{\mathbf{j}}_\mathbf{T} + (z_T^{\mathrm{FE2}/\mathrm{LR1}})_t\hat{\mathbf{k}}_\mathbf{T} \tag{A14}$$

For the case of coupled rotations, the components of the vectors expressed in the tibial coordinate system will continue to change even once a point on the rotational axis is selected because the tibial coordinate system is rotating as well. Therefore, the magnitude of Eqs. (A12) and (A13) must be used for the error function. Hence, FE1 and FE2 are positioned on the flexion-extension axis when the magnitudes of $(\mathbf{r_T^{FE1/LR1}})_t$ and $(\mathbf{r_T^{FE2/LR1}})_t$ do not change with time. Thus, $x_F^{\mathrm{FE1}/Fo}$, $z_F^{\mathrm{FE1}/Fo}$, $x_F^{\mathrm{FE2}/Fo}$, and $z_F^{\mathrm{FE2}/Fo}$ are iteratively adjusted until the change in $|\mathbf{r_T^{FE1/LR1}}|$ and $|\mathbf{r_T^{FE2/LR1}}|$ over time is minimized. The error functions E^{FE1} and E^{FE2} quantify the

changes in $|\mathbf{r}_T^{\mathbf{FE1/LR1}}|$ and $|\mathbf{r}_T^{\mathbf{FE2/LR1}}|$ as a root mean square error (Eqs. (A15) and (A16)). Here, n is the total number of data samples taken during flexion-extension of the tibia.

$$E^{\mathrm{FE1}} = \sqrt{\frac{1}{n}\sum_{i=1}^{n}(|r_T^{\mathrm{FE1/LR1}}|_i - |\bar{r}_T^{\mathrm{FE1/LR1}}|)^2} \tag{A15}$$

$$E^{\mathrm{FE2}} = \sqrt{\frac{1}{n}\sum_{i=1}^{n}(|r_T^{\mathrm{FE2/LR1}}|_i - |\bar{r}_T^{\mathrm{FE2/LR1}}|)^2} \tag{A16}$$

Thus, E^{FE1} is minimized by adjusting $x_F^{\mathrm{FE1}/Fo}$ and $z_F^{\mathrm{FE1}/Fo}$. Similarly, E^{FE2} is minimized by adjusting $x_F^{\mathrm{FE2}/Fo}$ and $z_F^{\mathrm{FE2}/Fo}$.

References

[1] Hicks, J., Arnold, A., Anderson, F., Schwartz, M., and Delp, S., 2007, "The Effect of Excessive Tibial Torsion on the Capacity of Muscles to Extend the Hip and Knee During Single-Limb Stance," Gait and Posture, **26**(4), pp. 546–552.

[2] Van Gheluwe, B., Kirby, K. A., and Hagman, F., 2005, "Effects of Simulated Genu Valgum and Genu Varum on Ground Reaction Forces and Subtalar Joint Function During Gait," J. Am. Podiatr. Med. Assoc., **95**(6), pp. 531–541.

[3] Fuchs, B., Kotajarvi, B. R., Kaufman, K. R., and Sim, F. H., 2003, "Functional Outcome of Patients With Rotationplasty About the Knee," Clin. Orthop. Relat. Res., **415**, pp. 52–58.

[4] Reinbolt, J. A., Haftka, R. T., Chmielewski, T. L., and Fregly, B. J., 2008, "A Computational Framework to Predict Post-Treatment Outcome for Gait-Related Disorders," Med. Eng. Physica, **30**(4), pp. 434–443.

[5] Besier, T. F., Lloyd, D. G., Ackland, T. R., and Cochrane, J. L., 2001, "Anticipatory Effects on Knee Joint Loading During Running and Cutting Maneuvers," Med. Sci. Sports Exercise, **33**(7), pp. 1176–1181.

[6] Besier, T. F., Lloyd, D. G., Cochrane, J. L., and Ackland, T. R., 2001, "External Loading of the Knee Joint During Running and Cutting Maneuvers," Med. Sci. Sports Exercise, **33**(7), pp. 1168–1175.

[7] Asano, T., Akagi, M., and Nakamura, T., 2005, "The Functional Flexion-Extension Axis of the Knee Corresponds to the Surgical Epicondylar Axis: In Vivo Analysis Using a Biplanar Image-Matching Technique," J. Arthroplasty, **20**(8), pp. 1060–1067.

[8] Edwards, M. L., 2000, "Below Knee Prosthetic Socket Designs and Suspension Systems," Phys. Med. Rehabil. Clin. N. Am., **11**(3), pp. 585–593.

[9] Incavo, S. J., Coughlin, K. M., Pappas, C., and Beynnon, B. D., 2003, "Anatomic Rotational Relationships of the Proximal Tibia, Distal Femur, and Patella: Implications for Rotational Alignment in Total Knee Arthroplasty," J. Arthroplasty, **18**(5), pp. 643–648.

[10] Most, E., Axe, J., Rubash, H., and Li, G., 2004, "Sensitivity of the Knee Joint Kinematics Calculation to Selection of Flexion Axes," J. Biomech., **37**(11), pp. 1743–1748.

[11] Besier, T. F., Sturnieks, D. L., Alderson, J. A., and Lloyd, D. G., 2003, "Repeatability of Gait Data Using a Functional Hip Joint Centre and a Mean Helical Knee Axis," J. Biomech., **36**(8), pp. 1159–1168.

[12] Lenz, N. M., Mane, A., Maletsky, L. P., and Morton, N. A., 2008, "The Effects of Femoral Fixed Body Coordinate System Definition on Knee Kinematic Description," ASME J. Biomech. Eng., **130**(2), p. 021014.

[13] Ramakrishnan, H. K., and Kadaba, M. P., 1991, "On the Estimation of Joint Kinematics During Gait," J. Biomech., **24**(10), pp. 969–977.

[14] Rivest, L. P., 2005, "A Correction for Axis Misalignment in the Joint Angle Curves Representing Knee Movement in Gait Analysis," J. Biomech., **38**(8), pp. 1604–1611.

[15] Hollister, A. M., Jatana, S., Singh, A. K., Sullivan, W. W., and Lupichuk, A. G., 1993, "The Axes of Rotation of the Knee," Clin. Orthop. Relat. Res., **290**, pp. 259–268.

[16] Churchill, D. L., Incavo, S. J., Johnson, C. C., and Beynnon, B. D., 1998, "The Transepicondylar Axis Approximates the Optimal Flexion Axis of the Knee," Clin. Orthop. Relat. Res., **356**, pp. 111–118.

[17] Asano, T., Akagi, M., Tanaka, K., Tamura, J., and Nakamura, T., 2001, "In Vivo Three-Dimensional Knee Kinematics Using a Biplanar Image-Matching Technique," Clin. Orthop. Relat. Res., **388**, pp. 157–166.

[18] Sonka, M., Hlavac, V., and Boyle, B., 1999, *Image Processing, Analysis, and Machine Vision*, Brooks-Cole, Pacific Grove, CA.

[19] DeLuzio, K. J., Wyss, U. P., Li, J., and Costigan, P. A., 1993, "A Procedure to Validate Three-Dimensional Motion Assessment Systems," J. Biomech., **26**(6), pp. 753–759.

[20] Windolf, M., Gotzen, N., and Morlock, M., 2008, "Systematic Accuracy and Precision Analysis of Video Motion Capturing Systems—Exemplified on the Vicon-460 System," J. Biomech., **41**(12), pp. 2776–2780.

[21] Blankevoort, L., Huiskes, R., and de Lange, A., 1988, "The Envelope of Passive Knee Joint Motion," J. Biomech., **21**(9), pp. 705–720.

[22] Johal, P., Williams, A., Wragg, P., Hunt, D., and Gedroyc, W., 2005, "Tibio-Femoral Movement in the Living Knee. A Study of Weight Bearing and Non-Weight Bearing Knee Kinematics Using 'Interventional' MRI," J. Biomech., **38**(2), pp. 269–276.

[23] Coughlin, K. M., Incavo, S. J., Churchill, D. L., and Beynnon, B. D., 2003, "Tibial Axis and Patellar Position Relative to the Femoral Epicondylar Axis During Squatting," J. Arthroplasty, **18**(8), pp. 1048–1055.

[24] Bach, J. M., and Hull, M. L., 1995, "A New Load Application System for In Vitro Study of Ligamentous Injuries to the Human Knee Joint," ASME J. Biomech. Eng., **117**(4), pp. 373–382.

[25] Martin, K. J., Neu, C. P., and Hull, M. L., 2007, "An MRI-Based Method to Align the Compressive Loading Axis for Human Cadaveric Knees," ASME J. Biomech. Eng., **129**(6), pp. 855–862.

[26] Durselen, L., Claes, L., and Kiefer, H., 1995, "The Influence of Muscle Forces and External Loads on Cruciate Ligament Strain," Am. J. Sports Med., **23**(1), pp. 129–136.

[27] Howell, S. M., Kuznik, K., Hull, M. L., and Siston, R. A., 2008, "Results of an Initial Experience With Custom-Fit Positioning Total Knee Arthroplasty in a Series of 48 Patients," Orthopedics, **31**(9), pp. 857–863.

[28] Banks, S., Bellemans, J., Nozaki, H., Whiteside, L. A., Harman, M., and Hodge, W. A., 2003, "Knee Motions During Maximum Flexion in Fixed and Mobile-Bearing Arthroplasties," Clin. Orthop. Relat. Res., **410**, pp. 131–138.

[29] Bingham, J., and Li, G., 2006, "An Optimized Image Matching Method for Determining In-Vivo TKA Kinematics With a Dual-Orthogonal Fluoroscopic Imaging System," ASME J. Biomech. Eng., **128**(4), pp. 588–595.

[30] Fantozzi, S., Leardini, A., Banks, S. A., Marcacci, M., Giannini, S., and Catani, F., 2004, "Dynamic In-Vivo Tibio-Femoral and Bearing Motions in Mobile Bearing Knee Arthroplasty," Knee Surg. Sports Traumatol. Arthrosc, **12**(2), pp. 144–151.

[31] Mahoney, O. M., Kinsey, T. L., Banks, A. Z., and Banks, S. A., 2009, "Rotational Kinematics of a Modern Fixed-Bearing Posterior Stabilized Total Knee Arthroplasty," J. Arthroplasty, **24**(4), pp. 641–645.

[32] Moro-oka, T. A., Muenchinger, M., Canciani, J. P., and Banks, S. A., 2007, "Comparing In Vivo Kinematics of Anterior Cruciate-Retaining and Posterior Cruciate-Retaining Total Knee Arthroplasty," Knee Surg. Sports Traumatol. Arthrosc, **15**(1), pp. 93–99.

[33] Sato, T., Koga, Y., and Omori, G., 2004, "Three-Dimensional Lower Extremity Alignment Assessment System: Application to Evaluation of Component Position After Total Knee Arthroplasty," J. Arthroplasty, **19**(5), pp. 620–628.

[34] Moro-oka, T. A., Hamai, S., Miura, H., Shimoto, T., Higaki, H., Fregly, B. J., Iwamoto, Y., and Banks, S. A., 2007, "Can Magnetic Resonance Imaging-Derived Bone Models be Used for Accurate Motion Measurement With Single-Plane Three-Dimensional Shape Registration?." J. Orthop. Res., **25**(7), pp. 867–872.

[35] Krackow, K. A., Bayers-Thering, M., Phillips, M. J., and Mihalko, W. M., 1999, "A New Technique for Determining Proper Mechanical Axis Alignment During Total Knee Arthroplasty: Progress Toward Computer-Assisted TKA," Orthopedics, **22**(7), pp. 698–702.

[36] Jessup, D. E., Worland, R. L., Clelland, C., and Arredondo, J., 1997, "Restoration of Limb Alignment in Total Knee Arthroplasty: Evaluation and Methods," J. South Orthop. Assoc., **6**(1), pp. 37–47.

[37] Weidenhielm, L., Wykman, A., Lundberg, A., and Brostrom, L. A., 1993, "Knee Motion After Tibial Osteotomy for Arthrosis. Kinematic Analysis of 7 Patients," Acta Orthop. Scand., **64**(3), pp. 317–319.

[38] Khan, R., Konyves, A., Rama, K. R., Thomas, R., and Amis, A. A., 2006, "RSA Can Measure ACL Graft Stretching and Migration: Development of a New Method," Clin. Orthop. Relat. Res., **448**, pp. 139–145.